Journal of Sound and Vibration (1997) **202**(2), 249–274

PREDICTIVE ACOUSTIC MODELLING APPLIED TO THE CONTROL OF INTAKE/EXHAUST NOISE OF INTERNAL COMBUSTION ENGINES

P. O. A. L. Davies and M. F. Harrison

Institute of Sound and Vibration Research, University of Southampton, Southampton SO17 1BJ, England

(*Received on* 8 *May* 1996, *and in final form* 27 *November* 1996)

The application of validated acoustic models to intake/exhaust system acoustic design is described with reference to a sequence of specific practical examples. These include large turbocharged diesel generating sets, truck engines and high performance petrol engines. The discussion includes a comparison of frequency domain, time domain and hybrid modelling approaches to design methodology. The calculation of sound emission from open terminations is summarized in an appendix.

1. INTRODUCTION

Intake and exhaust systems for reciprocating internal combustion engines are required to control sound emissions related to engine breathing within specified limits to comply with legislative targets, while ensuring that any related losses of engine power output and fuel efficiency are both kept to a minimum. Most contemporary design methodologies adopt some form of predictive modelling to achieve this aim. One such [1] is based on validated predictive modelling of sound propagation along the system and its component silencing elements [2–6] combined with appropriate descriptions [1, 7, 8] of the significant sources of excitation. Currently, sound propagation through the system is sufficiently well understood to ensure that sound transmission along intake and exhaust systems can usually be predicted with sufficient realism for any geometry, however complex. Corresponding predictive models for the sources do not yet exist, although the fluid dynamic processes concerned with flow generated sound have already been identified [7–12] for a sequence of specific cases.

Aerodynamic processes associated with the cyclic flow through the valves together with flow separation and vortex generation at junctions, expansions and the like provide significant sources of inlet and exhaust noise through transfers of mean or cyclic flow energy to wave energy [7–10]. The acoustic characteristics of the relevant duct system have a direct influence on both the efficiency and extent of such energy transfer, which may be modulated or amplified by acoustic resonance [11, 12]. Thus one finds that the associated noise emissions can be controlled or modified [1–7] by adopting appropriate acoustic or geometric design features, either to reduce the net energy transfer from the sources, or to attenuate selectively the dominant spectral components of the sound as it propagates through the system. In this context one should note that the individual system elements interact acoustically with each other, as well as with the sources.

The design objectives and constraints will depend to a varying extent on the specific application concerned: for example, whether this is a vehicle intake/exhaust system and

0022–460X/97/170249 + 26 $25.00/0/sv960842

subject to severe space constraints, or a system or design for fixed plant, where such restrictions may be less severe, but continuous high power output and fuel economy remain primary considerations. Also, when an extended production run of a single design is envisaged, such as is the case with a private passenger vehicle, where the development and testing of a sequence of prototypes is economically acceptable, but a high production cost per individual item is not; alternatively, where a restricted number of individual systems is concerned, such as for power generating plant, where first cost as well as operational economy is a prime consideration; finally, whether the design is concerned with a new installation for an existing engine, or whether an intake/exhaust system design for a completely new production engine is required.

Three representative examples of the application of predictive acoustic modelling in the context of intake/exhaust system design are described in section 4. The first is concerned with a 10 MW generating set exhaust system and was based on existing site measurements of noise emission and fuel economy. The second was concerned with the exhaust system development for a heavy truck engine running on a test bed, where acoustic modelling was employed to develop and then refine the acoustic performance of a sequence of prototype systems. The third was concerned with the development and evaluation of a new hybrid modelling technique for the prediction of intake/exhaust noise emission. In this case the predictions were compared with test bed measurements of noise emission by a high performance petrol engine with its production intake and exhaust systems, when it was run over an extended sequence of loads and speeds.

2. SOURCE/SYSTEM MODELS

Sound is radiated from intake and exhaust systems either from open terminations (snorkel or tailpipe noise) or from vibrating external surfaces driven by the internal pressure field (often referred to as shell noise). Before this can occur, the wave energy must travel along the system from the sources until it reaches those regions where it is emitted to the surroundings. Realistic descriptions of this overall acoustic behaviour, often called source/filter models, require that due account is included for the influence of the system boundaries on the transfer of acoustic energy from the sources and its subsequent transmission to the points of emission. For tailpipe or snorkel noise, for example, an equivalent acoustic circuit, with appropriate descriptions of any distributive features of the system elements, is often convenient for this purpose. With appropriate modifications, it can also be adopted to represent shell noise emission. In its simplest formulation, relevant to intake/exhaust acoustic modelling, the circuit represents wave propagation in one dimension (plane wave motion), with the subsequent sound radiation; otherwise an appropriate representation can be adopted for each propagating or relevant pressure mode. Normally the acoustic characteristics of the source and of the system it excites are both functions of frequency, so the discussion that follows here applies to each spectral component of a propagating mode.

Two representative source/filter acoustic circuit models are illustrated in Figure 1. In practical applications [1, 3] the acoustic properties of the filter correspond to those of the transfer element T combined with the termination element Z. The latter normally represents the acoustic impedance p_2/u_2 at the plane of external sound emission. With zero outflow the associated radiated sound power is then expressed by

$$W_r = 0{\cdot}5\sigma S_2 \,\mathrm{Re}\{p_2^* u_2\} = 0.5\sigma S_2 \,\rho_0 c_0 |u_2|^2, \tag{1a,b}$$

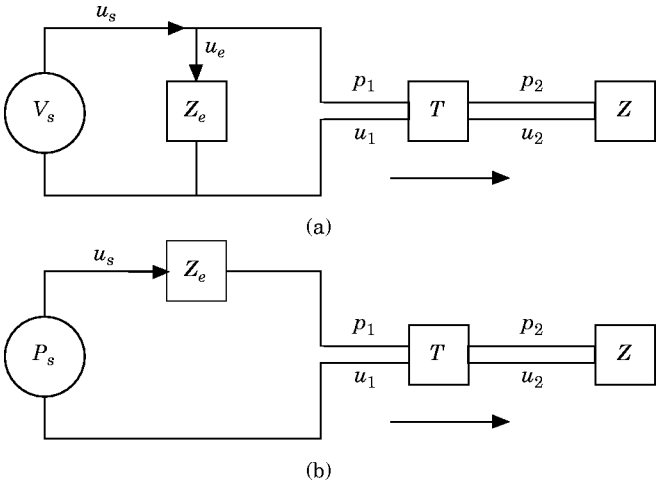

Figure 1. Acoustic circuits for intake/exhaust systems, excited by: (a) fluctuating mass or volume velocity; (b) fluctuating pressure or aerodynamic force.

where Re{ } denotes the real part, p_2^* is the complex conjugate value of the fluctuating pressure amplitude and u_2 is the amplitude of the acoustic particle velocity, with S_2 and σ, respectively, the associated surface area and acoustic radiation efficiency. A more extensive account of sound radiation from open terminations appears in the Appendix. When there is an outflow from the open termination at Mach number M, the ratio of mean flow velocity to the local sound speed, acoustic energy is also transported by the flow. With plane wave motion, the radiated sound power is then given by equation (A15).

A sequence of experimentally validated predictive models describing the spectral acoustic behaviour of acoustic filters, that have been developed to control acoustic transmission and radiation of piston engine breathing noise, are recorded in the literature. Some representative examples can be found in references [1–6]. They all demonstrate that their characteristic acoustic performance is governed by the transmission path geometry and the termination impedance Z, but remains independent of the characteristics of the source of excitation.

The source of Figure 1(a) represents one spectral component of fluctuating volume velocity with amplitude V_s, and associated effective shunt impedance Z_e; while Z_1, the corresponding input impedance of the filter at the source plane, is equal to p_1/u_1. This representation corresponds to fluctuating mass injection at the valves with an effective volume velocity $V_s = u_s S_s$, or that controlled by some equivalent aero-acoustic mechanism associated with separating shear layers, or that induced by vibrating surfaces. The shunt impedance Z_e includes, among other factors, the influence of the local acoustic environment on sound emission at the source. One notes too that the circuit model represents continuity of acoustic pressure with the source strength equated to the discontinuity in particle velocity $u_e = u_s - u_1 = p_1/Z_e$. In such terms it is equivalent to a point acoustic monopole in free space. The acoustic power output of this source is expressed by

$$W_m = 0{\cdot}5 \operatorname{Re}\{p_1^* V_s\} = 0{\cdot}5 |V_s^2| \operatorname{Re}\{Z_1/(1 + Z_1/Z_e)\}/S_s. \qquad (2a, b)$$

Alternatively, where the source is associated with fluctuating boundary stresses, the circuit model in Figure 1(b) represents continuity of particle velocity u_s across the source plane, with a source of strength $\partial f_s/\partial x$, where f_s is equated to the discontinuity of pressure

$(P_s - p_1)$ acting over area S_s, or $(P_s - p_1)S_s$. This equivalent to an acoustic dipole in free space. The acoustic power output is expressed by

$$W_d = 0{\cdot}5 \operatorname{Re}\{f_s^* u_s\} = 0{\cdot}5|f_s^2| \operatorname{Re}\{M_1\}, \tag{3a, b}$$

where the input mobility $M_1 = u_s/f_s = 1/Z_e S_s$, with $Z_e = (P_s - p_1)/u_s$. Here again, the series impedance Z_e includes the influence of the local acoustic environment. Analogous models can be derived for sources of mixing noise associated with shear layers, with appropriate integral expressions for non-uniform or extended source distributions that apply to shell noise. In any practical application the source of excitation may include a combination of these factors.

There is clear experimental evidence in the literature that the acoustical characteristics of the intake/exhaust system have a profound influence on their acoustic excitation by the breathing noise sources, as implied by equations (2b) and (3b). Similarly, measurements of the aerodynamic noise generated by the fluctuating drag forces produced by spoilers in low velocity flow ducts [9] have shown that the variation of observed sound power W scaled with flow velocity is according to $W \propto U^4 c^{-1}$ at frequencies at which acoustic propagation is restricted to plane waves, or below cut on, changing to $W \propto U^6 c^{-3}$, as for a free field dipole, at higher frequencies where multi-modal propagation can exist. The value of U giving the best collapse of all the data from several spoiler configurations was the mean velocity in the constricted flow past the spoiler. Other sequences of observations of the aerodynamic sound generated by a series of flow excited expansion chambers [7, 11, 13] at frequencies below cut on, also exhibited a similar sound power scaling law behaviour of around U^4. Matching the predicted spectral distributions based on acoustic circuit models [14] with the spectra reported in reference [11] showed that the associated aeroacoustic sources were predominately "dipole" in character. Recent measurements of flow noise generation in several engine exhaust systems and their component elements [15] provide further experimental evidence that is consistent with the other results described here.

2.1. ACOUSTIC WAVE PROPAGATION ALONG FLOW DUCTS

Acoustic plane wave transmission across an individual system component (element or discontinuity), or the sequence of components representing in the acoustic filter is also illustrated in Figure 1. With isentropic processes, the complex amplitude of each spectral component p^+ of the positively travelling and p^- of the negatively travelling component waves at frequency f are related to the corresponding fluctuating acoustic pressure p and acoustic particle velocity u by

$$p = p^+ + p^-, \qquad \rho_0 c_0 u = p^+ - p^-, \tag{4, 5}$$

where ρ_0 and c_0 are, respectively, the undisturbed density and sound speed in the medium and p, u, p^+ and p^- are all functions of axial position x along the duct and of frequency f.

It has been demonstrated [3] that equation (4) is valid irrespective of the existence or otherwise of a steady mean flow u_0, while equation (5) is similarly valid only as long as wave attenuation and dispersion by visco-thermal or other actions remain negligible. Thus alternative descriptions of the transfer may be expressed either in terms of fluctating pressures p_1 and p_2 with particle velocities u_1 and u_2 or in terms of the corresponding component amplitudes $p_1^{\pm}$, $p_2^{\pm}$. Thus plane wave acoustic transmission across the system, or a component across one or more of its elements, can be expressed in terms of the two corresponding transmission coefficients

$$T_i = p_1^+/p_2^+ \qquad T_r = p_1^-/p_2^-, \tag{6a, b}$$

together with a reflection coefficient, r, where

$$r = p_2^-/p_2^+, \qquad \text{or } r = (\zeta - 1)/(\zeta + 1). \tag{7a, b}$$

Here $\zeta = Z/\rho_0 c_0 = p_2/\rho_0 c_0 u_2$. Alternatively, the wave components $p_1^{\pm}$ on the source side of T can be related to $p_2^{\pm}$ on the load side by

$$p_1^+ = T_{11}p_2^+ + T_{12}p_2^-, \qquad p_1^- = T_{21}p_2^+ + T_{22}p_2^-, \tag{8a, b}$$

where T_{11}, T_{12}, T_{21}, and T_{22} are the four elements of the scattering matrix $[T]$ defining the transfer. The complex values of the four elements are functions of geometry, ρ_0, c_0, f and Mach number $M = u_0/c_0$, but remain independent of the value of Z. The transmission coefficients are related to the elements of $[T]$ by

$$T_i = T_{11} + rT_{12}, \qquad T_r = (T_{21}/r) + T_{22}, \tag{9a, b}$$

showing that T_i and T_r are both also functions of Z. However, the elements of $[T]$ and similarly T_i and T_r all remain independent of the source S, with acoustic excitation. Thus, logically, calculation of the characteristics of the acoustic filter should begin at the final acoustic load applied to the intake/exhaust system which is its open termination. This is described in the Appendix.

Since the elements T_{ij} of the scattering matrix remain independent of Z, they apparently provide the more elegant description of transfer characteristics, being often preferred for this reason. However, the transfer characteristics of flow duct components do not exhibit reciprocal acoustic behaviour [16], in contrast to the behaviour of linear electrical networks frequently adopted to represent them. Thus evaluation or measurement of realistic values of the matrix elements turns out to be a somewhat complex and exacting procedure, requiring a prior accurate determination of the transmission coefficients corresponding to the two distinctly different values of Z necessary for the solution of equations (9a) and (9b).

2.2. FINITE AMPLITUDE WAVE PROPAGATION ALONG FLOW DUCTS

When the fluctuating pressure amplitude exceeds the acoustic limit, so that the acoustic approximation ceases to be valid, the wave shape alters as it propagates, with a corresponding redistribution of the spectral component energies towards higher frequencies. Also, when the position and shape of the duct boundaries vary systematically or cyclically with time, spectral descriptions of wave propagation normally cease to be appropriate. Then any realistic description of the wave action must be formulated in time, even when the wave motion is periodic. A common analytic procedure for finite amplitude wave motion is based on the method of characteristics [17, see Chapter 10], or on equivalent solutions of the Euler and mass conservation equations. Time varying systems are normally analyzed in discrete time steps at appropriate time intervals. Many such systems can be treated as a time varying part coupled with a linear or acoustic part and the combination represented as a hybrid system; see Figure 2.

In the method of characteristics, see, for example, reference [17] the component waves $p^{\pm}(x, f)$ that describe one-dimensional wave motion in the frequency domain are replaced in the time domain by a small disturbance propagated along three characteristics (C_+, C_-, C_0) leaving a given point in the x–t plane. The equation of continuity and Euler's equation [3], with isentropic gas flow, can be cast in the form [17]

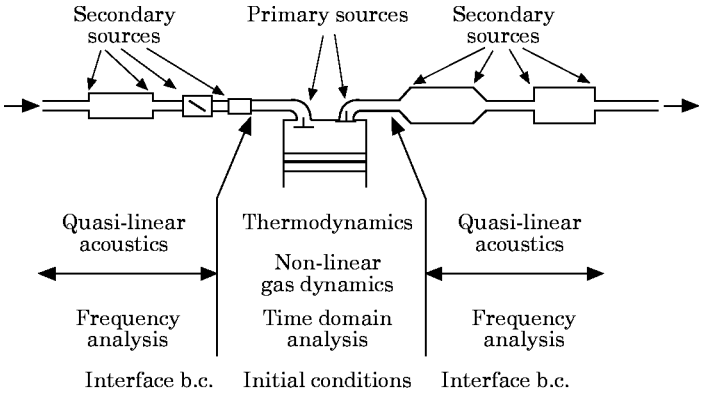

Figure 2. A hybrid prediction scheme with sources of excitation for piston engine breathing noise.

$$(\partial/\partial t + (v + c)\partial/\partial x)J_+ = 0, \qquad (\partial/\partial t + (v - c)\partial/\partial x)J_- = 0, \tag{10a, b}$$

where J_+ and J_- are, respectively, the Riemann invariants $v \pm \int \mathrm{d}p/\rho c$, and the differential operators acting on J_+ and J_- are the operators of differentiation along the characteristics C_+ and C_- in the x–t plane, while $v = u_0 + u(t)$, where $u(t)$ is the fluctuating velocity associated with the wave motion. Also, small perturbations of J_+ are propagated only along C_+ and those of J_- only along C_-. Furthermore, with isentropic flow, ρ and c are definite functions of p, so for a perfect gas

$$J_+ = v + 2c/(\gamma - 1), \qquad J_- = v - 2c/(\gamma - 1), \tag{11a, b}$$

where γ is the ratio of the specific heats of the gas.

With anisentropic flow, the equations of continuity and momentum cannot be cast in the form of equations (10a ,b) [3, 18] since $\mathrm{d}p/\rho c$ is not a perfect differential. These equations still permit [17] the separation of perturbations propagated along characteristics of one family. For such perturbations are in the form $\delta v \pm \delta p/\rho c$, and equations (10a, b) must be supplemented [3, 17, 18] by the adiabatic equation

$$(\partial/\partial t + v\partial/\partial x)s = 0, \tag{12}$$

which shows that small perturbations in the entropy δs are propagated along the characteristic C_0, which moves with the gas flow. The assignment of appropriate values to the Riemann invariants and to δs depends amongst other factors on the boundary conditions at the relevant points on the x–t plane.

Analytic procedures for modelling the gas dynamics associated with cyclic wave action in intake and exhaust, whether as isolated or as integrated systems, are well documented in the literature, since they have been subject to development and refinement throughout most of this century. Traditionally calculations start with the unsteady discharge from the cylinders through the valves and progress towards the open termination. The gas dynamics is modelled by the partial differential equations representing conservation of mass, linear momentum and energy transport and the fluid's constitutive equations or the equation of state, taken together with the geometrical and surface properties of the boundaries. They are then solved numerically by using a digital code representing the method of characteristics (MOC), the corresponding system of finite difference equations, or by some equivalent analytical procedure.

The successful and systematic application of such models to the design of slow running heavy diesel engines with improved output or performance [19] is well documented. But their corresponding lack of success to date in providing sufficiently realistic predictions of noise emission [20, 21] is also widely recognized. There are a number of well established reasons for this. A primary cause is the adoption of unrealistic boundary conditions for describing unsteady flow through the valves and both the time dependent wave transfer across and wave reflection from area and similar discontinuities that, with other geometrically complex elements, together form the essential physical features of practical intake or exhaust systems. Furthermore, though the models do set out to satisfy conservation of mass in the cylinder, they often fail to do so effectively throughout the intake, the exhaust downpipe, or the rest of the system [21]. For starting the calculations, existing procedures or codes often adopt ambient conditions for the initial values of pressure and temperature, with the fluid initially at rest. The calculations can then take of the order of hundreds of engine cycles [20] to converge satisfactorily. Arbitrary increase of wave damping to hasten such convergence [19] may yield time histories of the unsteady breathing characteristics that are satisfactory for engine performance estimates, but remain unrealistic for the prediction of noise emission. It is also widely recognized that flow noise generated at various points along the intake or exhaust system by shear layers and unsteady vortex shedding may make significant contributions to the emitted sound. As far as the authors are aware, existing codes [21] make no provision for the existence of such sources.

An alternative approach to the development of more realistic models depends on the successful formulation of a hybrid time/frequency domain simulation for the prediction of the acoustic as well as the overall performance of piston engine intake/exhaust systems. This adopts a time domain cycle to predict the instantaneous mass flow through the intake/exhaust valves, the method of characteristics, or its equivalent, to predict instantaneous pressure and particle velocities to the end, say, of the intake runner/exhaust downpipe and then frequency domain acoustics to propagate the pressure waves through the remainder of the system. Experience has shown [22, 23] that the correct handling of the time domain/frequency domain boundary has proved crucial for successful modelling of the observed behaviour.

2.3. BOUNDARY CONDITIONS

Since the gas dynamics of unsteady flow through constrictions and expansions is well established, realistic boundary conditions in relation to the flows through the valves might seem to present little difficulty in principle. For any practical case of current interest, however, the situation is somewhat more complex, since the relevant position of the rigid bounding surfaces at the valve change with time, as do the gas temperature and pressure in the cylinder as well as the pressure ratio across the valve, which normally lies above the critical value for sonic discharge during the initial part of the exhaust process. The problem is further complicated by flow separation with the time dependent changes in flow direction that exist during valve opening.

Realistic models describing finite amplitude wave reflection, and thus the boundary conditions at an open termination, do already exist and are also described in the Appendix. With the exception of some specific instances [20], corresponding realistic and experimentally validated models appropriate for all the other geometric features normally found with practical inlet and exhaust systems do not exist yet, to the authors' knowledge. For example, wave transmission and reflection with cyclically fluctuating finite amplitude waves were often found to differ significantly [20] from those predicted by the models adopted [19] for engine performance calculations.

However, acoustic characteristics such as impedance spectra, wave reflection and wave transmission spectra are readily derived, with well established and experimentally verified methods [2–6], for almost any complex geometry. An inverse Fourier transform of such frequency dependent wave reflection spectra, describing the corresponding wave reflection impulse function in the time domain, represents the boundary condition describing their influence on the remainder of the system. This provides a first approximation in general terms, but is more realistic for those system elements that behave as an acoustic filter. The validity of such procedures has been already demonstrated [22–24], for one group of relevant specific examples. One notes that acoustic characteristics are a function of gas temperature and composition [18] and of mass flow as well as of geometry, so may need updating accordingly as any calculation proceeds.

The boundary conditions at the interface between the time and frequency domain regions require constancy or matching in the time domain of the cyclically varying velocity $v(t)$ and pressure $P(t)$ across the interface. On the frequency domain side of the interface the values of $v(t)$ and $P(t)$ can be found by making an appropriate summation of the periodic harmonic components $u_0 + u(f)$ and $p_0 + p(f)$ of the acoustic fluctuations. To this end it is important that for each cyclic period T the frequency resolution $\delta f = N/T$ in the frequency domain corresponds to the time resolution $\delta t = T/N$ in the time domain, where N is a binary multiple of 256, say. The pressure reflection coefficient $r(f)$ can then be Fourier transformed to give the corresponding cyclic reflection coefficient $R(t)$ at the appropriate times. Upon recalling that $v(t) = u_0 + u(t)$ and noting that $P(t) = p_0 + p(t)$, after making use of equation (5), the relation between their fluctuating parts can be expressed by

$$p(t) = \rho_0 c_0 u(t)(1 + R)/(1 - R), \tag{13}$$

since, effectively, the flow conditions across the interface can be regarded as isentropic. Similarly, upon expressing the Riemann invariants in the alternate form [19]

$$\lambda = (c + (\gamma - 1)v/2)/c_0, \qquad \beta = (c - (\gamma - 1)v/2)/c_0, \tag{14a, b}$$

while the corresponding pressure ratio $P/p_0 = 0{\cdot}5(\lambda + \beta)^{2\gamma/(\gamma - 1)}$ at the appropriate times, the value of β corresponding to a value of λ incident at the interface can be expressed as

$$\beta = 2[1 + \rho_0 c_0 u(t)(1 + R)/\{(1 - R)p_0\}]^{(\gamma - 1)/2\gamma} - \lambda. \tag{15}$$

One notes that the relevant time averaged values u_0 and p_0 had already been established before the acoustic modelling of the filter was undertaken. Equation (15) now represents a time varying boundary condition at the relevant interface/discontinuity, in place of the time averaged conditions often adopted [19] hitherto.

The mean gas axial temperature distribution along exhaust ducts (and across expansion chambers) provides an additional condition which represents an essential factor in realistic acoustic modelling. Similarly, it represents the local baseline reference conditions along the downpipe, and thus is also an essential factor for realistic calculations of the wave motion by MOC or equivalent methods. The gas temperature distribution is a function of heat loss from the exhaust system surfaces to the surroundings and of any reactions occurring in the catalyst, when present; therefore it will depend on ambient conditions, engine speed and load, fuelling characteristics and so on. Thus it will be necessary to calculate all such relevant conditions for each of an appropriate range of representative vehicle or engine operating conditions.

3. INTAKE AND EXHAUST SYSTEM DESIGN STRATEGIES

Two alternative intake and exhaust design strategies are described in reference [1]. They both include sets of realistic validated models [2–6], with the associated software, to predict sound propagation in practical intake and exhaust systems and silencers, including the influence of geometry, temperature, mass flow and gas properties. The first alternative, which is illustrated in reference [1] by four practical examples, is concerned with the matching of system silencing performance, or its acoustic filter characteristics, to the relevant noise abatement requirements established by appropriate measurement. Thus it is assumed implicitly that the source characteristics remain effectively independent of changes in the acoustic filter characteristics of the system, which is apparently inconsistent with equations (2) and (3). Thus, this approach has been applied with most success to prototype exhaust system development with large turbocharged two- and four-stroke diesel engines running on a test bed, where the dominant sources are produced by the pulsating flow through the exhaust ports.

The second alternative design strategy, which is still under development, includes a systematic tuning of the system components that control or influence sound emision with an optimized matching of these to the engine operational and breathing characteristics that influence pollutant emissions, engine performance and fuel economy. This implies the adoption of an integrated prediction procedure which begins with the calculation of the cyclic wave action throughout intake, valves, cylinder and exhaust corresponding to all conditions of engine operation [22]. The valves, cylinder and manifolds together represent a time varying system, while it is assumed that the remainder of the intake and exhaust system acts mainly as a passive acoustic filter. The analysis of wave action in the time varying components of the running engine is best performed in time. However, realistic time domain descriptions of periodic wave action in all those parts of the system with complex geometry, such as acoustic filters and the like, do not currently exist [20, 21]. This situation is likely to continue as long as the representation of the relevant boundary conditions at area and other discontinuities along the flow path [19], including those associated with the sources of excitation, remain effectively time invariant and are thus either inadequate or inappropriate. In contrast to this, realistic spectral models of their acoustic behaviour are readily established. Since engine operation with the associated wave motion is cyclic, spectral representations are readily inverse Fourier transformed to the time domain, or the converse. This suggests a hybrid approach [22–24] to the calculation of integrated wave action throughout the system, as indicated in Figure 2, which also illustrates the type and notional positions of the acoustic sources. One should note that its successful application [22, 23] depends on the appropriate matching of wave reflection and propagation at the relevant hybrid interfaces.

This approach takes advantage of the existence of well established and documented methods [19] for calculating the cyclic thermodynamic and fluid dynamic processes in the cylinder with the associated wave action in the manifold in the time domain, together with the similarly well validated methods for calculating spectral descriptions of acoustic propagation in the remaining components of the intake and exhaust system. However, similarly well established methods [*loc. cit.*] are not yet readily available for calculating the contributions by any associated aeroacoustic sources with sufficient realism, either for the primary sources associated with the fluctuating flow through the valve ports, or the secondary sources associated with shed vorticity at relevant points along the flow path. Thus this somewhat neglected topic is now an active subject of research at the ISVR and also at a rather limited number of other establishments.

4. PRACTICAL EXAMPLES OF INTAKE AND EXHAUST SYSTEM DESIGN

The design strategy based on measured exhaust noise emission from the tailpipe is illustrated by two examples. The first concerns the redesign of the exhaust silencers for a new electric power generating plant powered by four 10 MW turbocharged diesel engines to meet specified environmental conditions. The second concerns a 350 HP turbocharged diesel truck engine while running on a test bed. In both cases narrow-band tailpipe noise spectra were measured under effectively free field conditions for appropriate ranges of running conditions.

The example presented to illustrate the hybrid predictive approach represents an investigation of the practical effectiveness of the modelling, rather than the development of a new design. In this case predicted narrow-band intake and exhaust noise emission spectra were compared with test cell measurements made on a four-cylinder high performance petrol injection engine equipped with its production intake and exhaust systems. Since frequency domain models of their acoustic characteristics were required for all the constituent elements of both systems, this represented a somewhat demanding test of the acoustic modelling with its predictive software, as well as that of the hybrid strategy. In all cases the acoustic performance and other calculations were carried out on a desk top computer (486 PC, or Macintosh SE30) with appropriate software developed by the authors. Run times for each calculation were typically 2–8 seconds for a spectrum with 512 components.

4.1. THE DIESEL GENERATING SET SILENCERS

The application of predictive modelling to the improvement of exhaust silencing performance is illustrated by the control of excessive noise emission by each ten megawatt turbocharged diesel generator of the set of four installed in the new power station. The engine of an electric generator is controlled to maintain a constant rotational speed, so the emitted noise spectrum consists of the same sequence of pure tones, although their relative amplitudes may vary with power output. The power station in this design study is on a restricted site, so a high attenuation per unit silencer volume was required at a number of specific frequencies.

Narrow band (0·5 Hz) spectral analysis of the noise emissions during initial trials, measured at 2 m from the open end of the exhaust tailpipe from engine 1, are reproduced in Figures 3(a) and 3(b); this is a single spectrum, divided into two parts for the readier visibility of detail. These observations show that the specified environmental limits, indicated by the dashed lines in the figures, are exceeded by some 20 dB at 29, 87·5 and 125 Hz and by 25 dB at 66·5 Hz, in particular, with lesser amounts at several other frequencies. The fixed firing frequency of the 16-cylinder Vee engine was 66·67 Hz at 500 rpm and one notes that several of the other dominant tones were not harmonically related to this frequency, but rather to the firing frequency of the individual cylinders, or to 4·167 Hz. The corresponding sequence of tones is clearly present in the spectrum, so that 29 Hz is at the seventh harmonic, 87·5 at the 21st and 125 Hz at the 30th. The amplitudes of the spectral components are related to the engine driving signal and its subsequent interaction with the filter characteristics of the silencer with its tailpipe, which was 102 m long.

An outline drawing of the original silencers appears in Figure 4(a); these were 2 m diameter, 8 m long cylinders; the positions of the 1·3 m diameter inlet and outlet pipes are shown. The silencer was divided into five sections by partial cross baffles at positions indicated by the dashed lines. The inner three sections were designed to act as reactive/resistive acoustic attenuators, while the outer two provided the required change

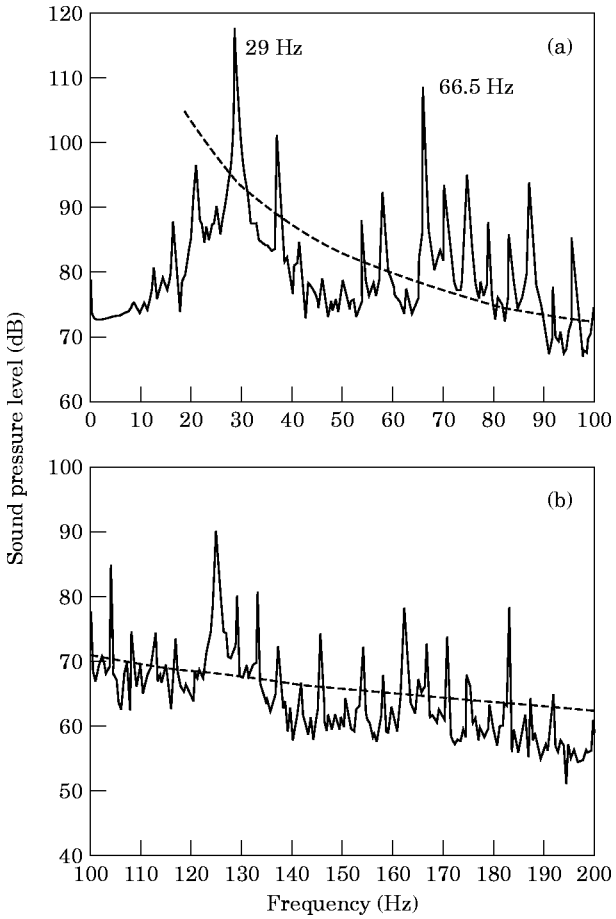

Figure 3. Stack noise spectra at 2 m for engine 1 with 9·6 MW output; – – –, estimated environmental limits at 2 m.

in gas flow direction at the silencer inlet and outlet. Site and installation restrictions did allow an increase in the length of the silencer by 1·8 m at the bottom and by about 1 m at the top, but not its diameter. The position of entry or exit of the main exhaust duct was obviously fixed, while economic considerations required that changes to the existing internal structure should be kept to a minimum. Appropriate modifications to the existing silencer were developed with the aid of predictive software that calculated the associated changes in acoustic attenuation performance under operating conditions. This was defined by an attenuation index, AL [3, 6], expressed by

$$AL = 20 \log_{10}|p_I^+ / p_O^+| = 20 \log_{10}|T_i|, \tag{16a, b}$$

where p_I^+ and p_I^- are, respectively, the predicted forward and backward travelling (incident and reflected) wave component spectral amplitudes at the silencer inlet plane, while p_O^+ and p_O^- are those at the outlet plane, and T_i for the conditions in Figure 1 is defined by equation (6a).

The development of the design changes was undertaken in a sequence of steps, each in close consultation with the client, and involving successively more extensive changes to the

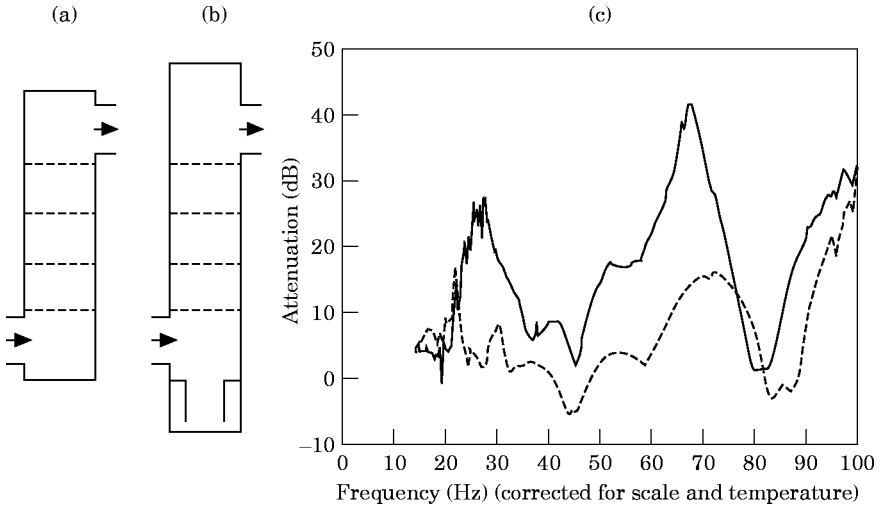

Figure 4. Validation of the proposed first stage silencer modifications for engine 1. (a) Existing silencer; (b) first stage modification; (c) measurements with 1/6 scale model silencers. ——, First stage modification; – – –, existing design.

original structure. Subsequently, the assessments of the resulting predicted improvements were validated at his request, by performing bench tests on a 1/6 scale model supplied by the client for acoustic testing in the laboratories at the ISVR. These tests included measurement of the spectral component wave amplitudes at the inlet and outlet planes of the model silencer unit by using the four microphone technique [6], in conjunction with white noise excitation. The resulting attenuation spectra were then adjusted to full scale and the designated operating temperature for comparison with the acoustic predictions. This involved adjusting for the change in sound speed in the exhaust gas at 315°C as well as the change to model scale. The resulting spectral scaling factor was then estimated as 4·27. Note that, to accommodate the model in the laboratory the length of the tailpipe was reduced to just under 1 m, corresponding to 5·26 m at full scale, rather than 102 m. This fact was taken into account during any comparisons between acoustic predictions and measurements made with the model, as well as any assessments of the likely performance up to 200 Hz at full scale. Since the uncertainties involved in such procedures increase with frequency, the attenuation comparisons presented here are confined to the first 100 Hz of the spectrum, adjusted to full scale operating conditions.

The first design change took full advantage of the free space available both at the top and of the bottom of the existing silencer. An outline drawing of the first modification to the silencer in Figure 4(b) shows the addition of a resonator tuned to 29 Hz at the bottom, that was predicted to provide an additional attenuation just in excess of 25 dB at that frequency, and an extension at the top to tune the associated side branch at the exit pipe to 66·5 Hz, also predicted to provide a similar increase of attenuation at the corresponding frequency. After they had been adjusted to full scale and operating temperature, spectral comparisons of the measured attenuation performance of the model, both before and following the first modifications illustrated in Figure 4(b), are presented in Figure 4(c). Clearly, these results confirm that the proposed improvements were achieved in the model silencer performance. They also demonstrate that there was also a gain of 18 dB in the performance at 87·5 Hz. Although it is not illustrated in the results presented here, there was a similar gain in the attenuation spectrum above 140 Hz. However, there was an

undesirable loss in attenuation performance of some 5 dB centred at 79 Hz, with a slightly greater unacceptable loss between 115 and 135 Hz and of some 16 dB at 125 Hz in particular, so further modifications were required.

Thus the silencing element in the central section was removed and its upper baffle modified to accommodate an annular quarter-wave side branch tuned to 125 Hz. This substantial reconstruction of the internal geometry was essential both to recover the lost performance associated with the first modification and to enhance that at 125 Hz. This new design of the central section gave a predicted increase of attenuation approaching 30 dB at 125 Hz, but also then reduced the predicted attenuation at 66·7 Hz by 3 or 4 dB, although it did not significantly alter that at 29 Hz. On the other hand, on the assessment of both the predictions at full scale and the results of the model tests indicated that there was a further gain of at least 10 dB over the original design in minimum attenuation throughout the spectrum, increasing to 30 dB between 100 and 165 Hz.

4.1.1. *Comparison of the results of the predictive modelling with the bench test and site measurements*

Working drawings describing the construction of the original silencers provided adequate detail for the predictive modelling of their acoustic performance under the prescribed operating conditions. With reference again to Figure 4(a), the flow path between the three central elements was via orifices in the baffle forming their lower surface, and hence through the walls of highly perforated pipes and finally through coincident holes in the baffle forming their upper surface. The central element had one such central tube with 46 per cent of its surface area open, while the adjoining pair were identical, with six such tubes distributed around the central inlet orifice, each having 20 per cent open surface area. The open tube surface to baffle orifice area ratio was respectively 1·5 or 2 in the two cases. Appropriate detailed procedures for deriving realistic models of the acoustical behaviour of all the elements concerned, both for the original and modified silencers, are available in references [2–6] and therefore are not repeated here.

The predicted attenuation of each of the model silencers was compared with that measured during the bench tests. Representative comparisons for the original silencer covering the spectral range 10–100 Hz are given in Figure 5(a), while the corresponding ones for the final design appear in Figure 5(b). The degree of agreement shown between predicted and measured attenuation is representative of that found at higher frequencies and for all the bench tests. The results clearly demonstrate that the modelling remains realistic, at least within the limits of the conditions for which these experimental results were obtained, suggesting that the bench tests were in fact superfluous, although perhaps reassuring for the client!

The noise emission measurements were repeated after the modified silencers had been installed. Comparison of the results of narrow-band (0·5 Hz) spectral analysis of these new measurements with those in Figure 3, combined with the results in Figure 5, provided estimates of the attenuation on site, or insertion loss increase produced by the modified silencers. The insertion loss estimates have also been included in Figure 5(b). Again, with two obvious exceptions at 29 and 87·5 Hz respectively, one can see that otherwise a close agreement between predictions and observations has been maintained. A likely explanation for these two exceptions is strong acoustic interaction, of the type expressed by equation (2), with the source of excitation at the first and third resonances of the chamber nearest the engine.

The insertion loss index IL is a popular description of acoustic performance, since it entails simply a measurement of the acoustic power W_1 radiated with the original exhaust

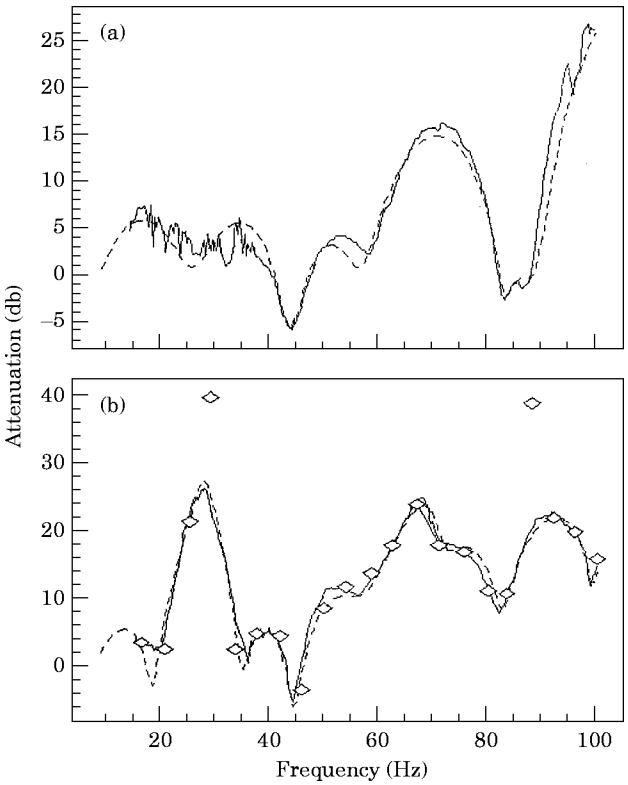

Figure 5. A comparison of predicted with measured attenuation: (a) original design; (b) final design. ——, measured with model; ---, predicted for model; ◇, measured on site, engine running.

system, followed by one of the corresponding power W_2 subsequent to the modifications, assuming that the engine running conditions remained otherwise the same. The insertion loss index is then [3] given by

$$IL = 10 \log_{10} W_1/W_2. \tag{17}$$

To compare such measurements with predictions, referring to Figure 1(a) one notes that $u_1 = u_s - p_1/Z_e$, and with the use of equations (4), (5) and (6) one can also show [8] that

$$p_2^+ = Z_e u_s/[(1 + \zeta_e)T_i + (1 - \zeta_e)T_r]. \tag{18}$$

The relation between the radiated power W and p_2^+ is given by equation (A15). Thus, to compare the predicted insertion loss with the measured value, one requires either appropriate spectral measurements or similar estimates of the source characteristics Z_e and u_s, or must assume they remain constant. They apparently must do so effectively to a fair approximation for most of the comparisons in Figure 5(b), but clearly do not for the two exceptions already noted.

Other measurements on the site boundary revealed that the loudest tone was still audible at 66·7 Hz, with a level that exceeded the hearing threshold of the normal ear by some 20 dB. Under normal environmental conditions one might expect that a pure tone at such a low level would remain well masked by the ambient acoustic climate. Thus, in terms of the original specification, the modified silencers performed satisfactorily. Additionally,

these measurements were also consistent with the results given in Figure 5(b), when these are compared with the original spectral levels recorded in Figure 3.

One notes further that the neglect of any source/filter coupling, such as that illustrated in Figure 1, or expressed by equations (2) and (3), was more or less justified in this case by the results. This was clearly fortuitous, as the strong interaction between the source and the first element of the silencer, or filter, was obviously beneficial in this instance. However, practical experience shows that this assumption is seldom realistic, especially in relation to high performance internal combustion engines currently installed in cars and commercial vehicles.

4.2. HEAVY TRUCK ENGINE SILENCER DESIGN

The application of predictive modelling to the development of an optimized exhaust silencer for a heavy truck is illustrated by the next example. This concerns the development of a high acoustic performance exhaust system [1] for noise control during the first Quiet Heavy Vehicle prototype development. It was aimed at determining the technical feasibility and cost of reducing the noise levels of heavy diesel engine goods vehicles to levels some 10 dB(A) lower than the then current values. Since engine surface noise presented a major problem in achieving this goal, it was decided to reduce exhaust noise emission to below the level at which its contribution was significant. Thus tailpipe noise emission was assigned an upper limit of 69 dB(A) at 7·5 m [25]. Furthermore, the combined engine/turbocharger performance was degraded when the maximum back pressure exceeded 45 mm of mercury, so this was specified as a maximum limit. The simultaneous satisfaction of these two requirements established the design criteria for the exhaust system.

Finding adequate space on a tractor unit for an exhaust system designed to meet this challenging specification presented an initial problem. Vehicle manoeuvrability precluded mounting it in the popular position behind the cab, and the only possible free space was below the front bumper. The final design that would fit within the only space available is illustrated in Figure 6(a). It consisted of two cylindrical boxes 0·25 m diameter and almost 2 m long. When the pipe bend near the turbocharger oulet is included, this layout required a total of four sharp bends, with their associated static pressure losses. To reduce the back pressure, the exhaust pipe diameter was increased from 100 to 125 mm at the entry to the 180° bend between the boxes, thus reducing the flow dynamic pressure by a factor of 2·4 both in the bend and the second box. The initial bend design included steady flow diffusion by distributing expansion uniformly around the bend, but in the final construction it was replaced by the abrupt expansion shown, with an associated increase in the overall system pressure loss from 25 mm Hg to 35 mm Hg.

As can be seen in Figure 6(a), the complete silencer system consisted of five chambers, each including one or two tuned quarter wave annular side branches. This gave a total of eight side branches with acoustic lengths arranged in geometric progression [1], either to cover the five octave bandwidth of the overall radiated exhaust noise spectrum, or to cancel the loss of attenuation associated with the half-wave resonances of the connecting pipes. The corresponding acoustic length of each side branch was its physical length plus an appropriate end correction [3], while the folded side branch in the second chamber represented a special case [1]. Due account was included in the predictive modelling for the influence of mean flow, axial and radial temperature gradients and exhaust gas composition.

As indicated in Figure 6(b), the preliminary measurements showed that the acoustic performance was severely restricted by internally generated flow noise, an expected result. This arose from reverberant amplification associated with the vortices [11] shed at each

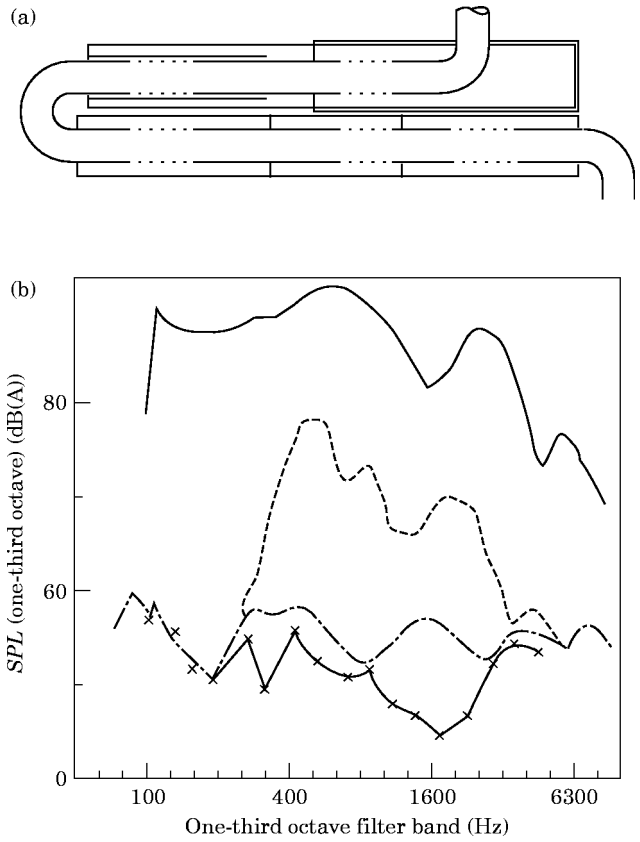

Figure 6. (a) The silencer design for the Foden QHV, showing perforated tube sections in extended inlet and outlet pipes (side branches). The first chamber of the first silencer is sheated with 3 mm asbestos and an outer layer of 1·2 mm thick aluminium sheet. (b) Test bed measurements at full load, adjusted to 7·5 m; averaged for eight speeds from 1000 to 2500 rpm. ——, Peak open pipe; – – –, omitting perforate brides (flow noise); ——, silenced, peak measured; –×–, peak predicted.

area expansion along the exhaust flow path. The vortex shedding was suppressed by bridging the gaps between the inlet and outlet pipes by lengths of perforated pipe as illustrated in Figure 6(a). Initially, the porosity of their walls, that is the ratio of hole or open area to total area, exceeded 20 per cent. Thus the acoustic impedance of the walls remained sufficiently low for them to behave as if they were acoustically transparent [6]. Observations demonstrate that as wall porosity is reduced below about 15 per cent, the resistive component of their acoustic impedance, which varies inversely with wall porosity, adds further useful damping to the side branch resonances. The consequent increase to their acoustic resonant bandwidth yields corresponding benefits to the broadband attenuation performance of the silencer.

The perforated tube sections bridging the openings between the pipe and expansion chambers also reduced the back pressure significantly as well as reducing flow noise. The relative influence of flow noise is illustrated in Figure 6(b) which compares three composite one-third octave band noise spectra measured at eight engine speeds with full load, with predictions calculated with the predictive software, after they have all been rescaled to 7·5 m. One should note too the good agreement between predicted and measured performance below 300 Hz, where the relative influence of flow noise is known to remain

small. With the optimized prototype design of silencer fitted, the maximum emitted exhaust noise levels at full load never exceeded 67 dB(A) at any of the speeds tested. However, this limiting value was increased to 69 dB(A) with the final operational version.

The choice of hole size and perforate porosity was found to have a significant influence both on acoustic performance and flow generated noise. Quantitative understanding of the former of these phenomena now exists [2, 6]. The best acoustic performance was obtained with small holes and high porosity. Also, both flow noise and pressure loss increased with hole size and porosity. However, a practical limit to the minimum acceptable hole size is provided by their tendency to clog with fouling during normal service. A fair compromise that was finally adopted had 3 mm dia holes with ten percent porosity, although the porosity was halved in one box for the operational version, leading to the 2 dB loss in performance noted above. The significant influence on silencer performance by fouling during service is described in reference [26], where it was strongly recommended that fouling should be removed by steam cleaning during regular maintenance, so that the acoustic performance is maintained.

4.3. HYBRID APPROACH TO PREDICTIVE MODELLING

Hybrid predictive modelling, illustrated in Figure 2, represents one of the contemporary design methodologies [22–24] for optimizing intake and exhaust system overall performance that are either currently available or in an advanced stage of development. The prediction of sound emission from a high performance petrol engine intake and exhaust system [21, 22] demonstrates the practical effectiveness of the hybrid approach to source/filter modelling. Relevant test data were available defining power output, mechanical, volumetric and thermal efficiencies, while valve design and manifold layout were already established. The approach adopted the assumption that the spectral distributions of the sound emitted were strongly controlled by the associated filter characteristics of the intake and exhaust, and were scaled in amplitude by the corresponding volume velocity through the valve ports. The implementation coupled a time domain treatment of the combustion in the cylinders and associated valve and manifold gas flows, with a frequency domain analysis for the filter characteristics of the remainder of the system. The interfacing required for this hybrid approach at the positions illustrated in Figure 2, is as described in section 2.3, and took advantage of the fact that the relevant operations were all cyclic, and so could be readily Fourier transformed from one domain to the other. Initially, the valve flow time histories were assumed to follow the variations in valve port area, being updated during the calculations to include better estimates of the conditions controlling the flow through the values at each instant in time. This should include taking due account of the period during each cycle during which the flow velocity through them attains the local sound speed, although this was not done with sufficient realism in the example described here, due to a current lack of a sufficiently refined model for this purpose. When due account of all the relevant features are not included, for example, as is likely with the adoption of empirically based time averaged discharge coefficients [19], the source modelling will certainly underestimate the contributions of the higher frequency components to the exhaust flow time history. The development of appropriate new models that provide more realistic estimates of the value flow time histories in all practical circumstances is obviously one significant component of current research.

The manifold geometry associated with each valve was different, requiring individual calculations for each cylinder. When an appropriate summation of the contribution from each of the four cylinders was included, these took a combined total of around 15 seconds to perform with a 486 model PC at each engine running condition. Some

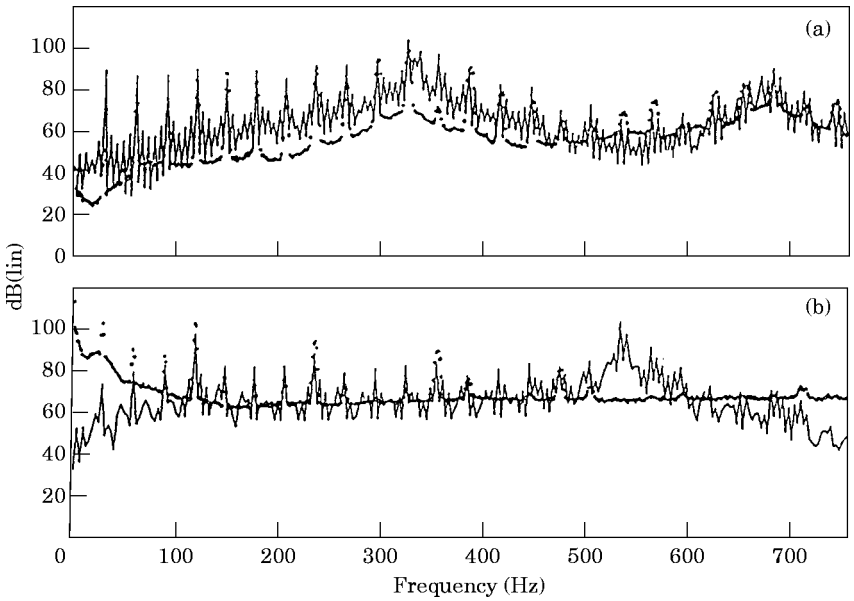

Figure 7. Intake and exhaust noise emission at 3600 rpm. Predictions by the hybrid method compared with measurements: (a) intake; (b) exhaust. ——, Predicted; • • •, measured.

typical results of the predicted combined noise emissions from the four cylinders are compared with the test cell measurements in Figure 7. Both the predicted and measured spectra are narrow-band and thus provide comparisons at each engine order. One should note too that test cell "cut-off" at around 150 Hz [22], meant that the validity of any comparisons was extremely doubtful below this frequency, while the continuous and rapid low amplitude oscillations in the predictions are obviously spurious and probably an artefact of the calculations. The spectral broadening of the measurements at higher frequencies is due to small engine speed fluctuations during each test. Above 150 Hz the intake predictions in Figure 7(a) clearly match the observations quite well, except for the one component at 350 Hz which was overpredicted. The exhaust noise predictions in Figure 7(b) are clearly in error above 500 Hz, due probably to the inadequacies in the description of the valve flow time histories described in the previous paragraph, while the hump in the spectra between 500 and 600 Hz occurred at all engine speeds and may represent some defect in the acoustic, or frequency domain modelling. Between 150 and 500 Hz, where the predictions are most realistic, the magnitude of the spectral peaks was consistently underestimated, also partly due perhaps to the neglect of secondary flow noise sources which may have been present. On the other hand, the spectral levels of the intermediate peaks was generally overpredicted. Even though systematic discrepancies existed, the comparisons were encouraging and indicated where the modelling could be improved by further studies.

5. DISCUSSION

Growing public concern for the environment, with the marketing advantage in the face of intense competition conferred by the rapid development and manufacture of high

quality products, has led to a growing realization that the development of equally effective design technology for the prediction and control of noise emissions by internal combustion engines and reciprocating compressors is equally urgent. Some examples of the incorporation of current predictive acoustic models into the design methodology presented here indicate some of the advantages that may result. Although effective in practical application in the first example, where the flow velocities were sufficiently low that flow noise generation within the exhaust system was not a problem, this was not the case with the other two examples. This is a consequence of the fact that experimentally validated predictive models describing sound propagation in exhaust systems have reached a relatively high stage of development, but the same is not yet true for the predictive modelling of the sources of excitation, including all significant aeroacoustic sources.

Two alternative modelling strategies were described both of which depend on similar validated models describing sound propagation through the relevant parts of the intake and exhaust system: that is, on the acoustic characteristics of the filter. Otherwise, they differ significantly, since the hybrid approach includes predictions of the primary source of excitation associated with the fluctuating mass flow through the valves, while the other does not. Thus it corresponds much more closely to the source/filter model in Figure 1(a) than does the frequency domain approach. Attempts to rectify this deficiency by measuring the source impedance of a running engine in the frequency domain [27], or similarly to characterize the source [27–29], have not in general produced consistently reliable predictions of noise emissions, except perhaps in a few specific instances. The result of one investigation [28] did demonstrate that the measured source spectrum was more sensitive to the acoustic characteristics of the exhaust system element adjacent to the exhaust valves, and was significantly less so for the remainder of the system. This observation is also consistent with the results recorded in Figure 6(b), and with the results and recommendations [1] recorded elsewhere. Despite this deficiency, frequency domain modelling has proved both useful and effective for a rational and systematic approach [1, 3] to initial and prototype system development [1, 25], since it provides substantial reductions in both the time and cost required compared with a purely experimental approach. Also its adoption can guide the achievement of an optimum acoustic performance [1] within the prescribed space and other practical limitations. A further practical advantage is that the associated software normally takes a few seconds to run on a standard desktop computer, so the results of any calculations are almost instantly available, facilitating performance assessment and leading to rapid prototype development.

Within the limitations just outlined, the frequency domain approach is clearly capable of realizing a satisfactory system design, so long as source/filter interaction is appropriately included (see Figure 5) and so long as flow noise remains insignificant or its contribution can be minimized (see Figure 6) by appropriate detail design of the flow path. In general it has proved more effective for the design of intake systems, since flow noise is then seldom a significant problem. However, it provides no guide to the concurrent optimization of engine output or fuel efficiency. There are now several alternative programmes in existence that potentially or actually undertake this task, see for example, references [21, 30], as well as providing predictions of noise emission by exhaust systems. They appear to require several hours to run with substantial computational facilities [20], to produce useful results. On the other hand, the hybrid approach [22] also has this potential, both for the prediction of sound emission and of engine performance. Furthermore, it currently provides somewhat more realistic predictions in a few seconds rather than hours, and runs on a desktop computer. When the envisaged developments in hybrid modelling are completed, the noise emission predictions should certainly become more realistic than those currently

available. However, it already offers a substantial advantage in terms of design office time and resources, and in particular for the enhanced facilities, such as the speed of response, that permit a rapid and systematic optimization of design detail to achieve a specific aim. In conjunction with an appropriate and perhaps extensive database, hybrid modelling also offers the possibility of predicting both the performance and acoustic emissions of a notional engine, during the concept development stage of a new vehicle or engine design.

It is clearly desirable that all the results of such calculations should be open to clear interpretation during system design or development. The fact that individual elements normally interact acoustically means that the relative contributions of the individual elements to the overall acoustic performance should be clearly identified, rather than their behaviour in isolation. Furthermore, the associated software should provide sufficient interactive facilities to provide physical insight into the relation between acoustic behaviour and the geometry or other relevant features of the system, or of its individual elements, as well as the consequence of any changes in detail. This is essential both to guide any optimization process, and to build up experience and thus develop expertise. Although the inclusion of appropriate optimization procedures in the software might be at first sight appear attractive [31], so far it has proved less effective in practical application [1] than a systematic approach carried out by suitably qualified and experienced design staff.

In this context, single parameter descriptions of the acoustic performance of the system or its constituent elements are often convenient [1–3, 6 8]. As well as insertion loss index IL and attenuation index AL defined in equations (17) and (16), respectively, they might also include spectral descriptions of radiated power and directivity (see the Appendix). Alternatively, one might adopt a sound power loss index WL, expressed for plane waves [6] by

$$WL = 10 \log_{10}(W_I/W_0), \tag{18a}$$

where

$$W_I = (S_I \rho_I c_I)[(1 + M_I)^2 |p_I^+|^2 - (1 - M_I)^2 |p_I^-|^2], \tag{18b}$$

in which S_I is the corresponding inlet cross-section area, while W_0 at its termination is evaluated by the relevant expression corresponding to equation (18b). Another commonly adopted performance parameter is the transmission loss index TL, which is identical with WL as long as the presence of both incident and reflected waves is included in the evaluation of W_I and W_0. However, in many published examples it is assumed that the termination remains anechoic, so that p_0^- is then always zero. In this case WL and TL must clearly differ.

One notes that the indices AL, WL, and TL are all independent of the source characteristics, and thus are readily evaluated with existing frequency domain models, while the insertion loss index IL is not. However, the measured insertion loss represents a more realistic description of overall source/system acoustic behaviour than do the other three, while the record demonstrates that there may be significant uncertainties involved in predictions of insertion loss by a purely frequency domain approach. Such is not the case with the hybrid approach, since this includes an evaluation of the frequency dependent source characteristics. Thus it has the potential for providing consistently realistic predictions of intake and exhaust noise emission that a purely frequency domain approach normally lacks. The record also demonstrates that the hybrid approach maintains corresponding advantages over those based solely on time domain modelling, not only in

terms of the time resolution and realism of the predictions, but also in terms of the relatively modest computational facilities required for the calculations.

At the present time and in the context of inlet and exhaust system noise emission modelling, the full potential of the predictive capabilities of all the current software is restricted by their inability to describe adequately all the associated contributions that may arise from the aeroacoustic sources. This fact is already widely recognized and is an active topic of current research at the ISVR.

REFERENCES

1. P. O. A. L. Davies 1996 *Journal of Sound and Vibration* **190**, 677–712. Piston engine intake and exhaust system design.
2. J. W. Sullivan 1979 *Journal of Acoustical Society of America* **66**, 772–788. A method for modelling perforated tube muffler components.
3. P. O. A. L. Davies 1988 *Journal of Sound and Vibration* **124**, 91–115. Practical flow duct acoustics.
4. P. O. A. L. Davies 1992 *ISVR Technical Report No*. 213, *University of Southampton*. Practical flow duct acoustic modelling.
5. P. O. A. L. Davies 1993 *Noise Control Engineering Journal* **40**, 135–41. Realistic models for predicting sound propagation in flow duct systems.
6. P. O. A. L. Davies, M. F. Harrison and H. J. Collins 1997 *Journal of Sound and Vibration* **200**, 195–225. Acoustic modelling of multiple path silencers with experimental validations.
7. P. O. A. L. Davies 1996 *Journal of Sound and Vibration* **190**, 345–362. Aeroacoustics and time varying systems.
8. P. O. A. L. Davies 1992 *ISVR Technical Report No*. 207, *University of Southampton*. Intake and exhaust noise.
9. P. A. Nelson and C. L. Morfey 1981 *Journal of Sound and Vibration* **79**, 263–289. Aerodynamic sound production in low speed flow ducts.
10. J. C. Hardin and D. S. Pope 1992 *American Institute of Aeronautics and Astronautics Journal* **30**, 312–317. Sound generation by stenosis in a pipe.
11. P. O. A. L. Davies 1981 *Journal of Sound and Vibration* **77**, 191–209. Flow acoustic coupling in ducts.
12. J. C. Bruggeman, 1991 *Journal of Sound and Vibration* **150**, 371–393. Self sustained aero-acoustic pulsations in gas transport systems.
13. J. D. Wu 1994 *M.Sc. Thesis*, *I.S.V.R.*, *University of Southampton*. Flow generated noise in piston engine intake and exhaust.
14. J. Takano 1994 *M.Sc. Thesis*, *I.S.V.R.*, *University of Southampton*. Flow noise prediction modelling of exhaust silencers.
15. J. Kunz and P. Garcia 1995 *SAE Technical Paper* 950546. Simulation and measurement of hot exhaust gas flow with a cold air flow bench.
16. P. O. A. L. Davies 1991 *Journal of Sound and Vibration* **151**, 333–338. Transmission matrix representation of exhaust system acoustic characteristics.
17. L. D. Landau and E. M. Lifshitz 1959 *Fluid Mechanics*, Oxford: Pergamon Press.
18. P. O. A. L. Davies 1988 *Journal of Sound and Vibration* **122**, 389–392. Plane acoustic wave propagation in hot gas flows.
19. R. S. Benson 1982 *The Thermodynamics and Gas Dynamics of Internal Combustion Engines*, *Volume I*. Oxford: Clarendon.
20. A. Onorati 1994 *Journal of Sound and Vibration* **171**, 369–395. Prediction of the acoustical performance of muffling pipe systems by the method of characteristics.
21. F. Payri, A. J. Torregrosa and M. D. Chust 1996 *Journal of Sound and Vibration* **195**, 757–773. Application of McCormack schemes to IC exhaust noise predictions.
22. M. F. Harrison 1994 *Ph.D. Thesis*, *I.S.V.R.*, *University of Southampton*. Time and frequency domain modelling of vehicle intake and exhaust systems.
23. M. F. Harrison and P. O. A. L. Davies 1994 *Proceedings of the Institute of Mechanical Engineers*, *CC*487/019, 183–190. Rapid predictions of vehicle intake/exhaust noise.
24. F. Payri, J. M. Desantes and A. J. Torregrossa 1995 *Journal of Sound and Vibration* **188**, 85–110. Acoustic boundary conditions for unsteady one-dimensional homentropic flow calculations.

25. J. W. Tyler 1979 *Proceedings of the Institute of Mechanical Engineers*, *London* **193**(23), 137–147. The TRRL quiet heavy vehicle project.
26. P. M. Nelson and M. C. P. Underwood 1982 *TRRL Supplementary Report* 746. Operational performance of the TRRL quiet heavy vehicle.
27. D. F. Ross and M. J. Crocker 1983 *Journal of Sound and Vibration* **90**, 491–508. Measurement of the acoustical internal source impedance of an internal combustion engine.
28. J. E. Temple 1980 *M.Sc. Thesis*, *I.S.V.R.*, *University of Southampton*. An investigation into the source region characteristics of internal combustion engine exhaust systems.
29. L. Desmonds, J. Hardy and Y. Auregan 1995 *Journal of Sound and Vibration* **179**, 869–878. Determination of the acoustical source characteristics of an internal combustion engine by using several calibrated loads.
30. S. M. Sapsford, V. C. M. Richards, D. R. Armlee, T. Morel and M. T. Chapple 1992 *SAE* 920686. Exhaust system evaluation and design by non-linear modelling.
31. R. J. Alfredson 1971 *Ph.D. Thesis*, *I.S.V.R.*, *University of Southampton*. The design and optimisation of exhaust silencers.
32. Lord Rayleigh 1894 *The Theory of Sound* (second edition). London: Macmillan; See articles 307–314.
33. C. L. Morfey 1969 *Journal of Sound and Vibration* **9**, 357–366. Acoustic properties of openings at low frequencies. See also ibid., 367–372. A note on the radiation efficiency of acoustic duct modes.
34. R. M. Munt 1990 *Journal of Sound and Vibration* **142**, 413–436. Acoustic transmission properties of a jet pipe with subsonic jet flow, I: the cold jet reflection coefficient.
35. H. Levine and J. Schwinger 1948 *Physical Review* **73**, 383–406. On radiation of sound from an unflanged circular pipe.
36. P. O. A. L. Davies and R. F. Halliday 1981 *Journal of Sound and Vibration* **76**, 591–594. Radiation of sound by a hot exhaust.
37. M. C. A. M. Peters, A. Hirschberg, A. J. Reijnen and A. P. J. Wijnands 1993 *Journal of Fluid Mechanics* **256**, 499–534. Damping and reflection coefficient measurements for an open pipe at low Mach and low Helmholtz numbers.
38. P. O. A. L. Davies 1987 *Journal of Sound and Vibration* **115**, 560–564. Plane wave reflection at flow intakes.
39. A. M. Cargill 1982 *Journal of Fluid Mechanics* **121**, 59–105. Low frequency sound radiation and generation due to the interaction of unsteady flow with a jet pipe.
40. P. O. A. L. Davies and J. J. Gu 1990 *Journal of Sound and Vibration* **141**, 165–166. Finite amplitude wave reflection at an open exhaust.

APPENDIX

A.1. SOUND EMISSION FROM OPEN TERMINATIONS

This topic is of considerable importance in the context of inlet and exhaust system acoustic modelling, but to the authors knowledge a collected account of it has not formed part of the relevant literature. It has been provided here to rectify this situation. Classical solutions describing sound emission and reflection from open terminations [32] represent the fluctuating acoustic velocity by an equivalent oscillating piston and treat the open end as a pressure release surface with an equivalent added fluctuating mass. In such analytic solutions for the radiation impedance, the presence of any time averaged flow through the open end has usually been neglected, so they apparently do not apply in a formal sense to flow ducts generally, although they represent a limiting condition. However, one can show that [4] due account for the influence of any such flow on both sound power emission or reflection may be included in the evaluation of the corresponding pressure reflection coefficient instead. On the other hand, one notes that [4] the flow does modify the directivity of the emitted sound field.

With plane waves incident on an open termination, the pressure reflection coefficient can be expressed as

$$r = p^-/p^+ = -R_M \exp(-2\mathrm{i}kl), \qquad \text{(A1a, b)}$$

where the modulus R_M represents the influence of the local geometry and mean flow with Mach number M on the pressure release characteristics, while l is an appropriate end correction representing the reactive influence of the associated fluctuating mass. Alternatively, one can express this as

$$r = \exp(-2\psi), \tag{A2}$$

where ψ is complex. The radiation impedance $Z_r = \rho_0 c_0(1 + r)/(1 - r)$ can be evaluated in terms of ψ by

$$Z_r = \rho_0 c_0 \tanh \psi = \rho_0 c_0(R_r - \mathrm{i}X_r), \tag{A3a, b}$$

where R_r and X_r are the real and imaginary parts, respectively, of the corresponding specific impedance ratio $\zeta_r = Z_r/\rho_0 c_0$.

A.2. RADIATION IMPEDANCE AND EFFICIENCY WITH ZERO MEAN FLOW

For the special case of an open-ended circular duct of radius a fitted with an infinite baffle (flange), the specific acoustic impedance ratio for the plane acoustic mode (Helmholtz number $ka < 1{\cdot}8$) is given [32] by

$$R_r = 1 - \mathrm{J}_1(2ka)/ka, \qquad X_r = \mathrm{S}_1(2ka)/ka, \tag{A4a, b}$$

where $\mathrm{J}_1(2ka)$ is the Bessel function of unity order of the first kind and $\mathrm{S}_1(2ka)$ the corresponding Struve function. The asymptotic values of R_r and X_r for small and large arguments are

$$R_r \to 0{\cdot}5(ka)^2, \qquad X_r \to 8(ka)/3\pi, \qquad \text{for } ka \to 0, \tag{A5a, b}$$

$$R_r \to 1, \qquad X_r \to 2/\pi ka, \qquad \text{for } ka \to \infty. \tag{A5c, d}$$

The corresponding radiated sound power W_r is expressed in terms of the fluctuating acoustic particle velocity u by

$$W_r = \pi(a)^2 \overline{u^2} \rho_0 c_0 R_r, \tag{A6}$$

where the overbar represents a time average. Since the simple harmonic fluctuations $\overline{u^2} = 0{\cdot}5|u|^2$, comparison with equation (1b) shows that the radiation efficiency σ is then equal to R_r. The result in equation (A4a) can be compared to the radiation efficiency for a small pulsating sphere, which is equal to $(ka)^2/(1 + (ka)^2)$.

When the open pipe is without a flange, the source strength is effectively halved as $k_a \to 0$ compared to that of the flanged case, since the relevant conductivity is doubled. The mean square pressure in the far field is also effectively halved for the same radiated power. It follows that the radiation efficiency is also halved, with resulting asymptotic values $\sigma = (ka)^2/4$, $ka \to 0$ and $\sigma \to 1$, $ka \to \infty$. Alternatively, Landau and Lifshitz [17], (art. 75) have derived an equivalent approximate expression valid for low Helmholtz numbers. They treated sound emission from a tube of cross-sectional area S as equivalent to sound emission from a pulsating body with surface motion Su. Their estimate of the emitted sound power W_L is then expressed as

$$W_L = \rho_0 S^2 \overline{\dot{u}^2}/4\pi c_0, \tag{A7}$$

where $\overline{\dot{u}^2}$ is the time averaged value of $(\mathrm{d}u/\mathrm{d}t)^2$. With simple harmonic motion $\dot{u} = \mathrm{i}\omega u$; this, when substituted in equation (A7), leads to

$$W_L = 0{\cdot}25\, \pi a^2 \overline{u^2} \rho_0 c_0 (ka)^2, \tag{A7a}$$

for a circular tube of radius a, yielding the same asymptotic value $\sigma = (ka)^2/4$, $ka \to 0$ as already expressed above. At moderate values of the Helmholtz number a useful approximation for σ for the unflanged open pipe is given by $(ka)^2/(4 + (ka)^2)$, yielding a value that is 2 per cent too large when $ka = 0{\cdot}5$, 6 per cent too large when $ka = 1$, or $ka = 1{\cdot}8$, with a maximum excess of 7·5 per cent when $ka = 1{\cdot}5$.

With other geometries [33] or with a mean inflow or outflow [1], the appropriate value of the radiation resistance and hence of the radiation efficiency can be calculated from either the corresponding pressure reflection coefficient [4] or the radiation impedance [33].

A.3. REFLECTION COEFFICIENTS FOR OPEN TERMINATIONS RADIATING INTO FREE SPACE

The pressure reflection coefficient for an open termination has been extensively studied both theoretically and experimentally to explain the observed behaviour of organ pipes, resonators and other duct terminations. It is also of direct interest in the present context, since it forms the obvious starting point for the calculation of the acoustic characteristics of any flow duct of current interest. The influence of a mean subsonic outflow on the reflection coefficient for sound transmitted through the open end of a circular pipe has been studied theoretically by Munt [34]. He compared his results with the corresponding theoretical solution with zero flow by Levine and Schwinger [35] and with other approximate solutions that included flow, as well as with several sets of measurements. An experimentally validated extension to hot outflows can be found in reference [36].

Spline fits to the results of Munt's calculations [1] can be expressed as a sequence of equations giving $R_M = f(ka, M)$, for specified ranges of the Helmholtz number ka and a given value of M. With zero outflow $M = 0$, similar fits were made to the solutions given by Levine and Schwinger [35]. The corresponding reflection coefficient R_0 for no flow with $0 < ka < 0{\cdot}2$ is

$$R_0 = [1 - \{4 - f_0(ka)\}\sigma]^{0{\cdot}5}, \qquad f_0 = (ka) = 3{\cdot}47(ka)^{1{\cdot}9738}, \tag{A8a, b}$$

where $\sigma = (ka)^2/(4 + (ka)^2)$. With $0{\cdot}2 < ka < 1{\cdot}5$ the corresponding expression [31] is

$$R_0 = 1 + 0{\cdot}01336ka - 0{\cdot}59079(ka)^2 + 0{\cdot}33576(ka)^3 - 0{\cdot}06432(ka)^4. \tag{A8c}$$

The corresponding end corrections with zero outflow [3] are closely approximated [1] by the empirical expressions

$$l_0/a = 0{\cdot}6133 - 0{\cdot}1168(ka)^2, \qquad ka < 0{\cdot}5, \tag{A9a}$$

$$l_0/a = 0{\cdot}6393 - 0{\cdot}1104ka, \qquad 0{\cdot}5 < ka < 2. \tag{A9b}$$

The available observations of end correction with outflow do not exhibit any significant variation with M, for $M < 0{\cdot}3$. With outflow at very low Mach numbers and in the limit of low values of the Helmholtz number [37] the acoustic behaviour is strongly influenced by the vortex motion associated with the separating shear layers shed from the circumference of the pipe.

As far as the authors are aware, there is no equivalent exact analytical solution for inflow. Observations indicate that the behaviour depends on whether the flow enters smoothly (e.g., via a bellmouth) or separates from the walls at entry forming a *vena contracta*. When this occurs the local Mach number is increased by the factor α_s with a value increasing from unity with smooth entry flow to around two with a sharp edged re-entrant or Borda intake. The pipe edges are often slightly rounded so that in such situations likely values for α_s may lie between 1·45 and 1·65. A close fit to many

observations of the reflection coefficient with inflow at Mach number M [38] is given by the empirical expression

$$R_M = R_0[(1 - \alpha_s M)/(1 - \alpha_s M)]^{0\cdot9}, \tag{A10}$$

with $\alpha_s = 1$, when the flow enters without separation. Observations also suggest that the end correction is diminished by inflow according to

$$l_M = l_0(1 - M^2). \tag{A11}$$

Reflection coefficients for square, rectangular or other regular shaped openings may be found in the literature; see for example, reference [33].

A.4. THE RADIATED SOUND FIELD INTO FREE SPACE

Sound radiation from an open end is always to some extent directional. With zero mean flow, the directivity factor for an open circular termination (oscillating piston) in an infinite flange at an angle θ to the axis [32] is then equal to $2J_1\,(ka \sin\theta)/(ka \sin\theta)$. For $ka = 1\cdot8$ this has a value of 0·81 for $\theta = \pi/4$ and 0·65 for $\theta = \pi/2$. The directivity is somewhat modified by mean flow, being influenced both by convection and the presence of shear layers. However, provided that the local geometry and the mean flow remain unaltered, the directivity factors of two identical outlets should remain the same at the same angle. The directivity of sound radiation from an unflanged open pipe with outflow is described in reference [39].

Since with zero flow, the directivity remains unity along the line of the duct axis, the fluctuating pressure along this line will be same as that emitted from a point source that has the same power. Substituting $p_2^+(1 - r)$ for $\rho_0 c_0 u$ in equation (A6), where p_2^+ is the amplitude of the component wave in the duct incident at the open termination with reflection coefficient r and then equating it to that for a point source, one obtains

$$W_r = 0\cdot5(\pi a^2)|p_2^+|^2|1 - r|^2\sigma/\rho_0 c_0 = 0\cdot5(4\pi a_r^2)|p_r|^2\rho_0 c_0, \tag{A12a, b}$$

where p_r is either the free field pressure in the radiated sound field at a point B that is at a radial distance a_r along the axis from the open termination, or that from an equivalent source in free field. The corresponding pressure transfer function $T_B = 20\log_{10}(|p_2^+|^2/|p_r|^2)$ is then found from

$$|p_2^+|/|p_r| = 2a_r/[a|1 - r|\sigma^{0\cdot5}]. \tag{A13}$$

Similarly, the pressure transfer function T_A from some point A in the duct to the open termination can also be expressed as $T_A = 20\log_{10}(|p_A|/|p_2^+|)$. In terms of the corresponding component wave transfer coefficients T_i and T_r, one can express p_A as $p_2^+(T_i + rT_r)$, so that

$$|p_A|/|p_2^+| = |T_i + rT_r|. \tag{A14}$$

It is normal practice to calculate T_i and T_r starting from the open termination, at which a convenient value for $|p_2^+|$ is unity.

A.5. SOUND RADIATION FROM AN ENGINE EXHAUST

Cargill [39] extended Munt's solution for sound radiation from a jet pipe with cold subsonic outflow to hot flows. For the plane waves the acoustic power incident at the open end of the pipe [3] is given by

$$W_I = 0\cdot5(1 + M)^2|\overline{p_2^+}|^2/\rho_0 c_0.$$

With $M \to 0{\cdot}1$ and cold flow, one obtains an approximate prediction [36] for the proportion of the incident power that is radiated, which is

$$W_r/W_i = \{|1 - r|^2/(1 + M^2)\}\{(ka)^2/[4 + (ka)^2]\}. \tag{A15}$$

This expression gives predictions that agree with Munt's calculated values [39], with $ka < 1{\cdot}5$ and $M < 0{\cdot}5$.

With hot exhaust flow [36, 39], where the speed of sound is c_J and the density ρ_J, discharging into free space, where the ambient values are respectively c_0 and ρ_0, the ratio of radiated to incident sound power becomes

$$\frac{W_r}{W_i} = \frac{|1 - r|^2}{(1 + M_J)^2} \frac{(Kka)^2}{4 + (Kka)^2} \frac{\rho_0 c_0}{p_J c_J} \frac{[1 + 1/3(M_R)^2]}{[1 - (M_R)^2]^3}, \tag{A16}$$

where $K = c_J/c_0$, $M_R = (u_J - u_0)/c_0$ and u_0 is the velocity of any local external flow parallel to the exhaust pipe. This result has been experimentally validated [36] for Helmholtz numbers $ka < 0{\cdot}3$, $M < 0{\cdot}2$ and $K \leqslant 1{\cdot}5$. If one sets $K = 1$, equation (A16) provides predictions which also agree with Munt's calculated values to better than 2 per cent for the more extensive range $ka < 0{\cdot}4$, $M < 0{\cdot}5$.

When the exhaust system is a simple uniform pipe, the wave amplitude may be such that the acoustic approximation ceases to be valid. Under these circumstances the relevant reflection coefficient [40] is expressed by

$$J^-/J^+ = -1 + 0{\cdot}4M - 0{\cdot}08M^2 + 0{\cdot}016M^3, \tag{A17}$$

after including terms up to third order in the instantaneous flow Mach number M. Equation (A17) has been experimentally validated [40] over the range $-0{\cdot}2 < M < 0{\cdot}5$.

A.6. THE RADIATED SOUND FIELD INTO REVERBERANT OR SEMI-REVERBERANT SPACE

In the analysis so far it has been assumed that the sound is radiating into free space. There exists some evidence in the literature (see, for example, reference [37]), together with some experimental evidence among the authors' measurements (see, for example, Figure 7), that indicates that the reflection coefficient at an open termination can be significantly influenced by the presence of standing waves in the space into which the radiation takes place. Presumably, there is a corresponding influence on the sound power emitted and also on its directivity. For example, it is clearly recognized that the presence of reflecting surfaces in the vicinity of the exhaust/intake open termination (i.e., the ground plane), in what is otherwise free space, give rise to a local standing wave field. Similarly, there are many practical instances where the local vehicle structure acts as a somewhat "leaky" enclosure with a corresponding reverberant field. Since the acoustic behaviour of intake/exhaust systems is strongly influenced by their termination conditions, this is clearly a topic of practical concern. As far as the authors are aware, the relevant information in the literature hardly exists, and thus this remains a subject of scientific and practical interest that requires systematic investigation to quantify the influence of such reverberant fields on the acoustic behaviour of open terminations. This also represents an area of uncertainty in the application of test bed measurements to the prediction of sound emissions under what would normally be a different operating environment.